Monte Carlo Simulation of Total Radial Distribution Functions for Interlayer Water in Li-, Na-, and K-Montmorillonite Hydrates

Sung-Ho Park* and Garrison Sposito

Geochemistry Department, Earth Sciences Division, Mail Stop 90/1116, Lawrence Berkeley National Laboratory, Berkeley, California 94720

Received: August 24, 1999; In Final Form: February 22, 2000

Recent $^1H/^2D$ isotopic-difference neutron diffraction experiments on interlayer water in the two-layer hydrates of Wyoming montmorillonite with Li^+ or Na^+ counterions have shown that the organization of the water molecules differs from that in the bulk liquid. Monte Carlo simulations were performed to investigate molecular mechanisms underlying these structural differences in terms of radial distribution functions for H−O and H−H spatial correlations. Our simulations of the first-order difference total radial distribution function, $G_H(r)$, for interlayer water were in good agreement with published experimental data based on $^1H/^2D$ isotopic-difference diffraction patterns for the two-layer hydrates of Na- and Li-montmorillonite. Detailed examination of our results showed that the H−O and H−H spatial correlations found among interlayer water molecules differ from those obtained in the bulk liquid. Moreover, O−O spatial correlations are longer-ranged than in the bulk liquid because of cation solvation effects. A Monte Carlo simulation of $G_H(r)$ for the two-layer hydrate of K-montmorillonite predicted differences from those of the other two montmorillonite hydrates that should be observable by neutron diffraction.

1. Introduction

Smectites are layer-type aluminosilicates (clay minerals) with the atomic structure of mica,[1] but they are less well-crystallized than mica because of their random and incomplete pattern of isomorphic substitutions of metal cations for Si^{4+} and Al^{3+} in the layer structure. The nanoscale particles typical of smectites[1] thus have lower layer charges than particles of mica, and they readily undergo cation-exchange[2] and interlayer swelling[3] processes governed by the electrical double layer which forms on their basal planes in aqueous media. Smectites are ubiquitous in terrestrial weathering environments and play an important role in soil chemistry.[2] They are widely used in petroleum production, industrial catalysis, and radioactive waste disposal.[3,4] An understanding of their surface reactivity is essential to facilitating improved design for these commercial and environmental applications.

Spectroscopic studies of smectite hydrates[2,5] suggest that water molecules and cations that become intercalated between the clay layers take on configurations reminiscent of concentrated aqueous electrolyte solutions. These latter systems have been investigated very successfully over the past two decades by isotopic-difference neutron diffraction,[6,7] which recently has been applied to the study of interlayer water structure in hydrated smectites.[8−10] The experimental strategy in this technique is to expose the location of a diffracting atom more precisely in relation to its neighbors by making isotopic substitutions that create major differences in the pattern of coherent neutron scattering.[6] In their investigation of hydrated montmorillonite (a common smectite), Powell et al.[8−10] applied this approach with $^1H \rightarrow {}^2D$ substitution in the interlayer water. Their latest results[10] lend further support to the ionic solution picture[5] of the interlayer region.

* Address correspondence to this author at the following E-mail address: spark@nature.berkeley.edu.

The principal structure quantity investigated by Powell et al.[8−10] is the total radial distribution function,[6,11]

$$G(r) = \sum_{\alpha} \sum_{\beta} c_\alpha c_\beta b_\alpha b_\beta [g_{\alpha\beta}(r) - 1] \qquad (1)$$

whose Fourier transform is linearly related to the intensity of coherent scattering as measured in a neutron diffraction experiment. Here, c_α is the atomic fraction of an atom of species α in a diffracting system, b_α is its coherent scattering length, and $g_{\alpha\beta}(r)$ is a partial radial distribution function, which gives the relative probability that a β atom resides within a volume element centered at the distance r from an α atom centered at the origin of coordinates, with $g_{\alpha\beta}(r) \approx 1.0$ when no spatial correlation exists between atoms α and β.[12] Thus, $G(r)$ gives a relative probability for coherent neutron scattering by atoms located nonrandomly at the distance r from other atoms in a diffracting system. As applied to neutron diffraction by interlayer water using H/D isotopic substitution,[8−10] α,β = D, H, O, M, H2, Si, Al, Mg, or O2, where D, H, and O refer to interlayer D_2O or H_2O, M refers to the interlayer cation, and H2, Si, Al, Mg, and O2 refer to unsubstituted hydrogen, silicon, aluminum, magnesium, and oxygen in the clay mineral structure.

Sposito et al.[13] very recently reported a theoretical calculation of $G(r)$ for interlayer water in the two-layer hydrates of Na- and K-montmorillonite, based on Monte Carlo simulations of the partial radial distribution functions in eq 1 as obtained using the simulation methodology developed by Chang et al.[14] Their simulated $G(r)$ for the two-layer hydrate of Na-montmorillonite was in good qualitative agreement with $G(r)$ determined experimentally by Powell et al.[8] in showing that it differed significantly from $G(r)$ for bulk liquid water. However, the partial radial distribution functions calculated by Sposito et al.[13] did not include interlayer cations or those in the clay mineral structure, and it made no distinction between O and O2. Oxygen

10.1021/jp993017g CCC: $19.00
Published on Web 04/21/2000

in H_2O and O in the clay mineral structure were combined together in the calculation of $g_{\alpha\beta}(r)$, with atom β being both O and O2, and atom α being either H or O in an interlayer water molecule. This latter procedure may be questioned on the grounds that $g_{\alpha\beta}(r)$ in eq 1 has a different weighting (c_β) for different β atoms, such that the composite partial radial distribution function calculated by Sposito et al.[13] would not give the same contribution to $G(r)$ as a simple sum of the contributions from $g_{\alpha O}(r)$ and $g_{\alpha O2}(r)$. In this paper, we report new Monte Carlo simulations of interlayer water in two-layer hydrates of montmorillonite for which this important distinction between the two types of O atoms is made, and both interlayer and clay mineral cations are included. We compare our results quantitatively with the most recently published experimental $G(r)$ data[9,10] for the two-layer hydrates of Li- and Na-montmorillonite.

2. Simulation Methods

2.1. Radial Distribution Functions. Calculation of the total radial distribution function requires values for the coherent scattering lengths (b_α) and atomic fractions (c_α). The coherent scattering lengths for H, D, O, Li, Na, K, Si, Al, Mg, H2, and O2 are[15] −3.74, 6.67, 5.81, −1.90, 3.63, 3.67, 4.15, 3.45, 5.38, −3.74, and 5.81 fm, respectively. The atomic fractions of the atoms in our simulation cell can be calculated with the formula

$$c_\alpha = \frac{\alpha \text{ atoms per simulation cell}}{518} \quad (2)$$

where the denominator represents the total number of atoms in our Monte Carlo simulation cell, which includes eight unit cells of unhydrated Wyoming-type montmorillonite (326 atoms),[14]

$$M_6[Si_{62}Al_2](Al_{28}Mg_4)O_{160}(OH)_{32} \quad (M = Na, Li, \text{ or } K) \quad (3)$$

plus 192 atoms in 64 interlayer water molecules. Therefore, the water content of the montmorillonite hydrates is 8.0 H_2O or D_2O per unit cell. The chemical formula given in eq 3 is equivalent to that assumed by Powell et al.[8−10] for their Wyoming montmorillonite samples, whose water contents ranged from 6.2 to 10.3 H_2O per unit cell.

Powell et al.[10] determined the first-order difference total radial distribution function $G_H(r)$ for interlayer water after performing H/D isotopic-difference neutron diffraction experiments. This function is obtained from eq 1 by setting α = D, β = D, O, M, Si, Al, Mg, H2, O2, and α = H, β = H, O, M, Si, Al, Mg, H2, O2 successively, then subtracting the two resulting $G(r)$:[10]

$$\begin{aligned} G_H^h(r) = {} & c_H^2(b_D^2 - b_H^2)[g_{HH}(r) - 1] + \\ & 2c_Hc_O(b_D - b_H)b_O[g_{HO}(r) - 1] + \\ & 2c_Hc_{H2}(b_D - b_H)b_{H2}[g_{HH2}(r) - 1] + 2c_Hc_{O2}(b_D - \\ & b_H)b_{O2}[g_{HO2}(r) - 1] + 2c_Hc_{Mg}(b_D - b_H)b_{Mg}[g_{HMg}(r) - 1] + \\ & 2c_Hc_{Al}(b_D - b_H)b_{Al}[g_{HAl}(r) - 1] + 2c_Hc_{Si}(b_D - \\ & b_H)b_{Si}[g_{HSi}(r) - 1] + 2c_Hc_M(b_D - b_H)b_M[g_{HM}(r) - 1] \end{aligned} \quad (4)$$

where M = Li, Na, or K. Table 1 lists values of the coefficients in eq 4 used in our calculations for the three montmorillonite hydrates.[10,15] The corresponding first-order difference total radial distribution function for bulk liquid water is

$$\begin{aligned} G_H^w(r) = A\{ & c_H^2(b_D^2 - b_H^2)[g_{HH}(r) - 1] + \\ & 2c_Hc_O(b_D - b_H)b_O[g_{HO}(r) - 1]\} \end{aligned} \quad (5)$$

TABLE 1: Coefficients[10,15] Used in $G_H(r)$ for the Two-Layer Hydrates of Na-, Li-, and K-Montmorillonite and for Bulk Liquid Water (Units of mbarns, 1 mbarn = 0.1 fm²)

coefficient	value	coefficient	value
$c_H^2(b_D^2 - b_H^2)$	14.5	$2c_Hc_O(b_D - b_H)b_O$	28.7
$2c_Hc_{O2}(b_D - b_H)b_{O2}$	104.4	$2c_Hc_{H2}(b_D - b_H)b_{H2}$	−11.2
$2c_Hc_{Mg}(b_D - b_H)b_{Mg}$	2.0	$2c_Hc_{Al}(b_D - b_H)b_{Al}$	9.7
$2c_Hc_{Si}(b_D - b_H)b_{Si}$	24.1	$2c_Hc_{Li}(b_D - b_H)b_{Li}$	1.1
$2c_Hc_{Na}(b_D - b_H)b_{Na}$	2.0	$2c_Hc_K(b_D - b_H)b_K$	2.1

where A is a scale factor that can be determined by imposing the boundary condition,[10] $G_H^w(0) = G_H^h(0)$. Given the values of the coefficients listed in Table 1 and the boundary condition $g_{\alpha\beta}(0) = 0$, the values of A are 4.01, 4.03, and 4.03 for Li-, Na-, and K-montmorillonite, respectively.

The partial radial distribution functions used in eq 4 were calculated by Monte Carlo simulation. The partial radial distribution functions used in eq 5 were taken from experimental results published by Soper et al.,[16] who studied bulk liquid water by isotopic-difference neutron diffraction of D_2O/H_2O mixtures. Local coordination numbers $N_{\alpha\beta}(\rho)$ were calculated using the partial radial distribution functions in a conventional expression:[6a,12,13]

$$N_{\alpha\beta}(\rho) = 4\pi\frac{N_\beta}{V}\int_0^\rho g_{\alpha\beta}(r)r^2 dr \quad (6)$$

which gives the number of β atoms found within a spherical radius ρ around an α atom. Since the partial radial distribution function $g_{\alpha\beta}(r)$ approaches 1 at large r in an isotropic system,[6a,13] $G(r)$ in eq 1 approaches zero, implying no observable coherent scattering between two atoms far apart. Thus the total radial distribution function $G(r)$ must be interpreted as an angularly averaged quantity for systems with constrained geometry such as clay interlayers.[13]

2.2. Simulations. Monte Carlo (MC) simulations of montmorillonite hydrates were carried out on Cray J90 supercomputer clusters at the National Energy Research Scientific Computing Center using MONTE, a Metropolis Monte Carlo simulation code developed and extensively tested with successful results for clay mineral hydrate systems.[14] All MC simulations were performed in a constant ($N\sigma T$) ensemble, where absolute temperature (T) and the pressure applied normal to the clay layers (σ) are kept constant at 300 K and 100 kPa, respectively.

The model potential function used to represent the interactions montmorillonite−montmorillonite, montmorillonite−water, counterion−counterion, counterion−water, and water−water is given by

$$U(r_{ij}) = \sum_{i=1}^{N}\sum_{j\neq i}^{N}\left[\frac{q_iq_j}{r_{ij}} - A_{ij}e^{-B_{ij}r_{ij}} + C_{ij}e^{-D_{ij}r_{ij}}\right] \quad (7)$$

The effective charges (q) for the atoms on sites in water molecules and in the clay layer, and the van der Waals parameters (A, B, C, and D) describing short-range interactions between atoms in the water−cation−clay systems, are listed in Tables 2 and 3, respectively.[17−19] The water−water interaction is represented by the MCY potential,[20] whereas cation−water potentials are represented by MCY-type parametrization of the ab initio model of Bounds.[21] Detailed evaluations of eq 7 and its parameters in Tables 2 and 3 for use in clay−water systems have been reported by Skipper and his collaborators.[17−19]

The simulation cell used is a 21.12 Å × 18.28 Å patch with two half-layers of a Wyoming-type montmorillonite. This cell was replicated infinitely in three dimensions to mimic a

TABLE 2: Effective-Charge Parameters for Electrostatic Interactions in Eq 7[17−19]

atom	$q(e)$	atom	$q(e)$
O (T_d apical)	−1.0	(O)H (water)	0.71748
O (surface)	−0.8	Si (T_d)	1.2
O(H) (clay)	−1.7175	Al (T_d)	0.2
O(H) (water)	−1.43496	Al (O_h)	3.0
(O)H (clay)	0.7175	Mg (O_h)	2.0

TABLE 3: van der Waals Parameters for the Short-Range Interactions in Eq 7[17−19]

sites	A_{ij} (kcal mol^{-1})	B_{ij} (Å^{-1})	C_{ij} (kcal mol^{-1})	D_{ij} (Å^{-1})
		Water−Water		
H−H	0.0	0.0	666.33	2.7608
H−O	273.59	2.2333	1455.4	2.9619
O−O	0.0	0.0	1088213	5.1527
		Water−Clay		
H−Si	2.137	1.22	577.23	2.15646
H−Al	2.137	1.22	577.23	2.15646
O−Si	1345.8	2.2671	13061	3.2037
O−Al	1345.8	2.2671	13061	3.2037
		Water−Cation		
H−Li	741.667	2.5527	6662.279	3.51582
O−Li	192.957	1.32063	14169.718	3.65143
H−Na	884.2297	1.923886	2051.8654	2.3609517
O−Na	25.948129	0.77461042	61888.035	4.0849070
H−K	48.6581	1.63326	28317.87	3.60219
O−K	67.2407	1.009606	63754.99	3.485559
		Cation−Clay		
Si−Li	0.0	0.0	151.009	1.411
Al−Li	0.0	0.0	151.009	1.411
Si−Na	1505.4412	1.86517	2164.45	2.120855
Al−Na	1505.4412	1.86517	2164.45	2.120855
Si−K	0.0	0.0	1635.0237	1.96877
Al−K	0.0	0.0	1635.0237	1.96877

physically observable macroscopic system. Short-range interactions were treated with the all-image convention and a 9-Å real-space cutoff. Long-range electrostatic (Coulombic) interactions across (or beyond) the simulation cell were computed by the Ewald sum method.[14] The choice of a nanoscale simulation cell with periodic boundary conditions has been found to be successful in studying the structural and diffusive properties of clay−water systems.[14]

The simulation strategy we followed has been described and discussed in detail by Chang et al.[14] and Sposito et al.[13] Briefly, for the first 50 000 MC steps, only interlayer water molecules were allowed to move while the counterions and the clay layers (initial d spacing, 16 Å) stayed at their original positions. For the next 50 000 MC steps, water molecules moved and the clay layer was allowed to move only in the direction normal to the basal planes. For the next 100 000 MC steps, water molecules, the interlayer cations (Na^+, Li^+, or K^+), and the clay layers were allowed to move freely, with the upper clay layer moved one step in any (x, y, or z) direction with respect to the bottom layer for every five move attempts with the interlayer water molecules. In the next 2 500 000 MC steps, the same conditions as for the previous 100 000 MC steps were applied. The last 500 000 MC steps with 1000 realizations were used for output analysis. Data were collected every 500 steps for this 500 000-step run.

The partial radial distribution function (RDF) of each atomic pair in the system was collected for data analysis in terms of a $G(r)$ calculation, while the layer-spacing and potential energy profiles were monitored as typical indicators of system equilibration.[12,14] Data for the partial RDFs were obtained directly from the output of MONTE. Partial RDFs obtained from our previous simulation[13] of bulk liquid water, when constrained to the equilibrium density, show excellent agreement, in terms of peak positions and heights, with the partial RDFs for bulk liquid water obtained from neutron diffraction experiments by Soper et al.[16] This good agreement attests to the accuracy of the model water−water potential function.

TABLE 4: Intermolecular Coordination Numbers in Bulk Liquid Water and in Montmorillonite Interlayer Water

N_{OO}	r_{min} (Å)	N_{HO}[a]	r_{min} (Å)	N_{HH}[a]	r_{min} (Å)
		Bulk Liquid Water[b]			
5.40	3.50	1.02	2.50	5.3	2.95
		Li-Montmorillonite			
5.69	3.65	1.31	2.40	5.02	3.20
		Na-Montmorillonite			
5.68	3.70	1.34	2.40	5.11	3.20
		K-Montmorillonite			
5.71	4.00	1.36	2.50	4.40	3.20

[a] Intramolecular contributions (1.0 for N_{HO} and N_{HH}) have been subtracted from the value of the integral in eq 6. [b] From refs 13 and 16.

3. Results and Discussion

Simulated partial RDFs describing O−O, D−O, and H−H spatial correlations in interlayer water for Li-, Na-, and K-montmorillonite are compared to their experimental counterparts for bulk liquid water[16] in Figures 1, 2, and 3, respectively. Differences in peak heights and minima depths between interlayer and bulk water RDFs reflect the differences in N_β/V for these two systems, as can be seen readily from the definition of $g_{\alpha\beta}(r)$,[6a,13]

$$dn_{\alpha\beta} = 4\pi \frac{N_\beta}{V} g_{\alpha\beta}(r) r^2 \, dr \tag{8}$$

where $dn_{\alpha\beta}$ is the average number of β atoms within a spherical shell of radius r and thickness dr enclosing an α atom placed at $r = 0$, and N_β is the total number of β atoms in the system of volume V. For two systems to exhibit equal values of $dn_{\alpha\beta}$, the values of $g_{\alpha\beta}(r)$ must scale inversely with the number density N_β/V, and this is what occurs for interlayer water vs bulk liquid water in Figures 1−3. Because the bulk liquid would completely fill the simulation cell volume,[13] whereas interlayer water occupies only about one-third of our simulation cell volume, the remainder being occupied by clay layers, the values of N_β/V necessarily differ. This scaling effect notwithstanding, the partial RDFs give evidence for an organization of interlayer water molecules that is significantly different from the local tetrahedral coordination that is characteristic of bulk liquid water.[16,22] For example, strong oxygen−oxygen spatial correlations in interlayer water extend over a greater distance for the Li- and Na-montmorillonite hydrates than in liquid water (Figures 1 and 2), as indicated by the rather sharp second-neighbor peaks near 4 Å in $g_{OO}(r)$ and the broad third-neighbor peaks near 5.4 Å, neither of which are seen for liquid water. This kind of structure in $g_{OO}(r)$ is not observed in the K-montmorillonite hydrate (Figure 3), suggesting, therefore, that strong cation solvation effects are important in organizing interlayer water molecules. The fact that the first minimum in $g_{OO}(r)$ occurs at a larger r-value and the nearest-neighbor O−O coordination number is larger than in bulk liquid water (Table 4) substantiates the view of interlayer water as deviating from the local tetrahedral coordination in the bulk liquid, despite the greater degree of spatial ordering in the former.[23]

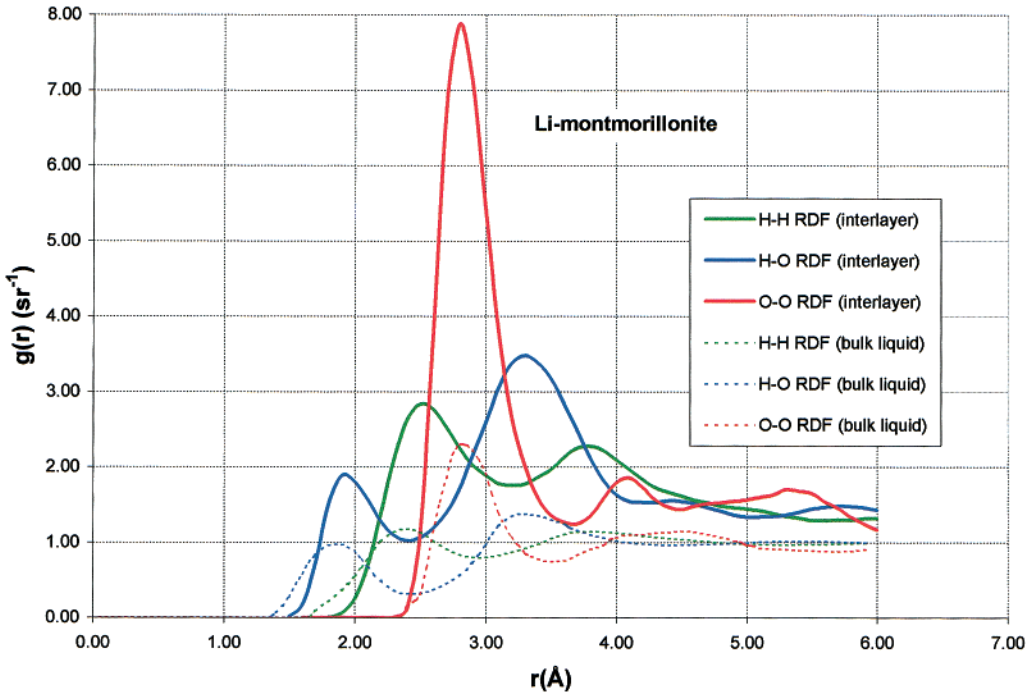

Figure 1. Partial radial distribution function for hydrated Li-montmorillonite as calculated by MC simulation (solid lines), and for bulk water as obtained from neutron diffraction[16] (dashed lines).

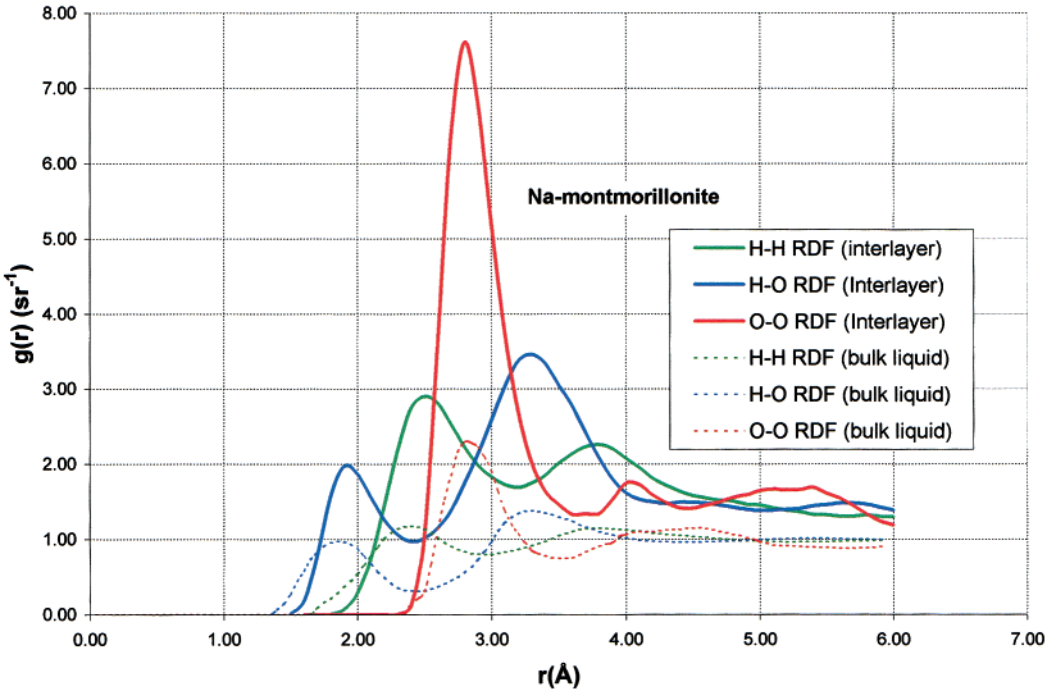

Figure 2. Partial radial distribution function for hydrated Na-montmorillonite as calculated by MC simulation (solid lines), and for bulk water as obtained from neutron diffraction[16] (dashed lines).

Hydrogen−oxygen spatial correlations in interlayer water as epitomized in $g_{HO}(r)$ also extend over larger distances than in the bulk liquid, indicating longer hydrogen bonds [first peak in $g_{HO}(r)$]. The nearest-neighbor H−O coordination number lies well above 1.0 (1.32 ± 0.02, Table 4), the value expected for perfect tetrahedral coordination of water molecules through hydrogen-bonding and that found in bulk liquid water. This result shows further that coordination among the interlayer water molecules is not bulk-liquid-like. Powell et al.[10] also measured a value of 1.3−1.4 for N_{HO} in the two-layer hydrate of Li-montmorillonite, but they attributed its difference from 1.0 to possible error due to peak overlap. We do not believe this type of error occurred in our calculation, suggesting therefore that their experimental result may be accurate. Similar differences from bulk water, but of opposite sign, exist for N_{HH} (Table 4), and its substantial drop in the case of the K-montmorillonite hydrate may reflect the greater role of the clay mineral surface in organizing interlayer water when a weakly solvating counterion is present.[14,24] If this attribution is correct, then the disrupting effect of the clay mineral surface on tetrahedral coordination among water molecules would appear to be even greater than that of cation solvation.

Figures 4 and 5 provide comparisons, for Li- and Na-montmorillonite, respectively, between the experimentally de-

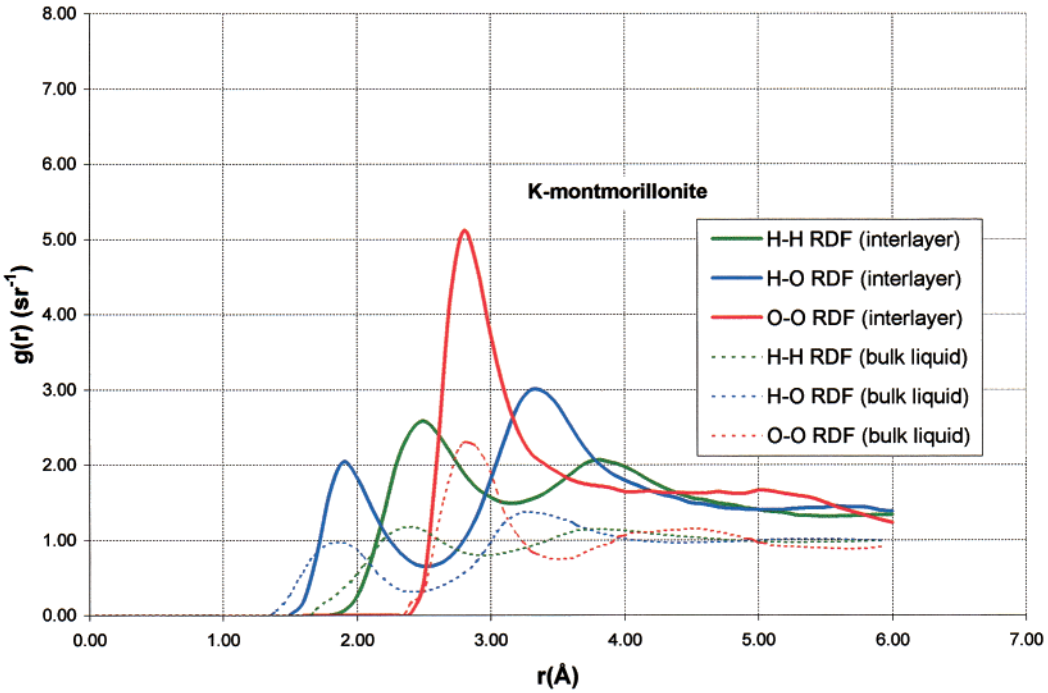

Figure 3. Partial radial distribution function for hydrated K-montmorillonite as calculated by MC simulation (solid lines), and for bulk water as obtained from neutron diffraction[16] (dashed lines).

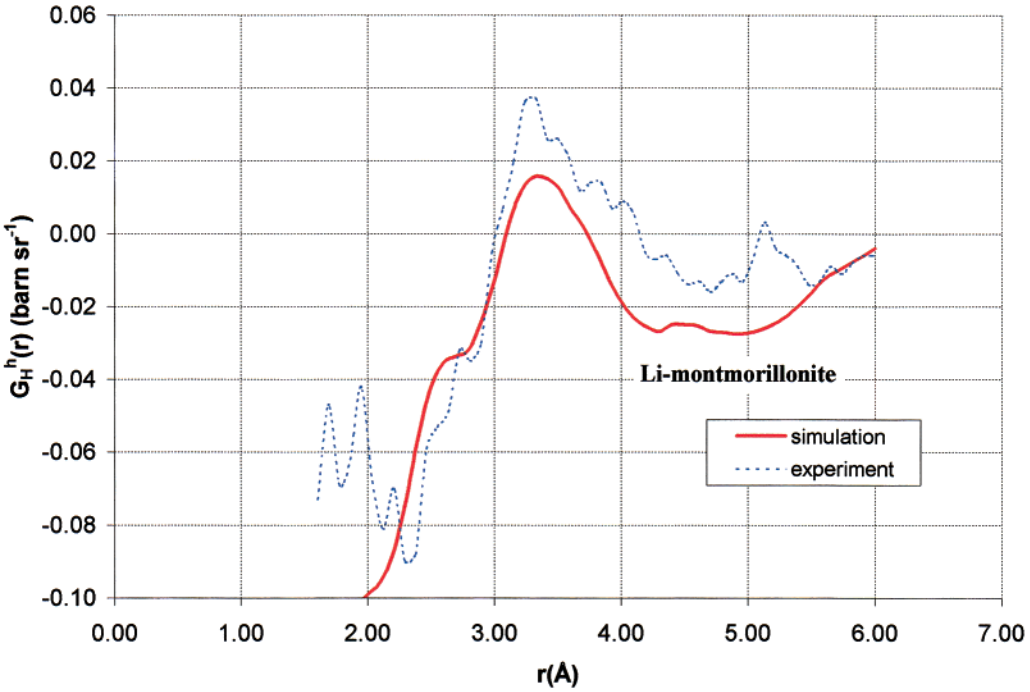

Figure 4. Total radial distribution function of the two-layer hydrate of Li-montmorillonite. MC simulation results (solid line) and isotopic-difference neutron diffraction results[10] (dashed line) are compared.

termined $G_H^h(r)$ based on the isotopic-difference neutron diffraction data of Powell et al.[8,10,25] and our simulated first-order difference total radial distribution function for interlayer water, calculated with eq 4, the numerical coefficients in Table 1, and the partial RDFs (full curves) in Figures 1 and 2. The agreement of the simulated $G_H^h(r)$ with the measured $G_H^h(r)$ is mostly within the experimental precision of the latter. The difference between experiment and simulation for 4 Å $< r <$ 5 Å may be the result of our model potential function producing stronger H−H and H−O correlations among interlayer water molecules than actually exist. In the bulk liquid, essentially no spatial correlations occur for $r >$ 4 Å (Figure 2, dashed curves).

Figure 6 shows the simulated $G_H^h(r)$ for interlayer water in the three montmorillonite hydrates as compared to a scaled $G_H^w(r)$ calculated with eq 5 and the coefficients in Table 1 using the experimental partial RDFs reported by Soper et al.[16] Compared to the two-layer hydrates of Li- and Na-montmorillonite, $G_H^w(r)$ displays a much more pronounced peak at $r = 2$ Å, noted also by Powell et al.,[10] but implies a more evident decline in H−H and H−O spatial correlations for $r >$ 4 Å (i.e.,

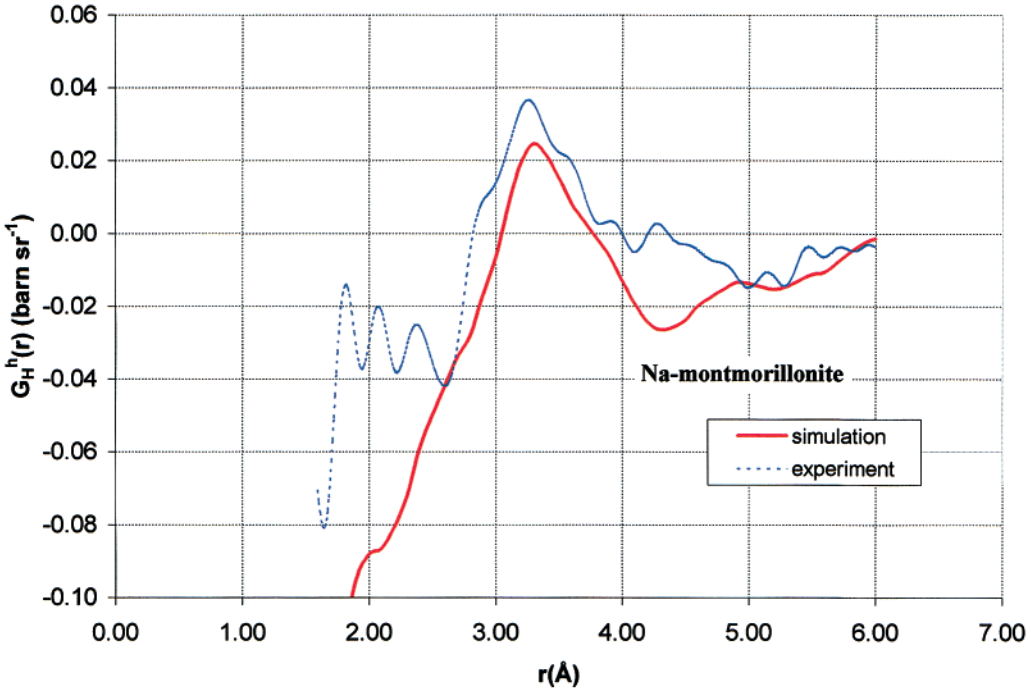

Figure 5. Total radial distribution function of the two-layer hydrate of Na-montmorillonite. MC simulation results (solid line) and isotopic-difference neutron diffraction results[8,25] (dashed line) are compared.

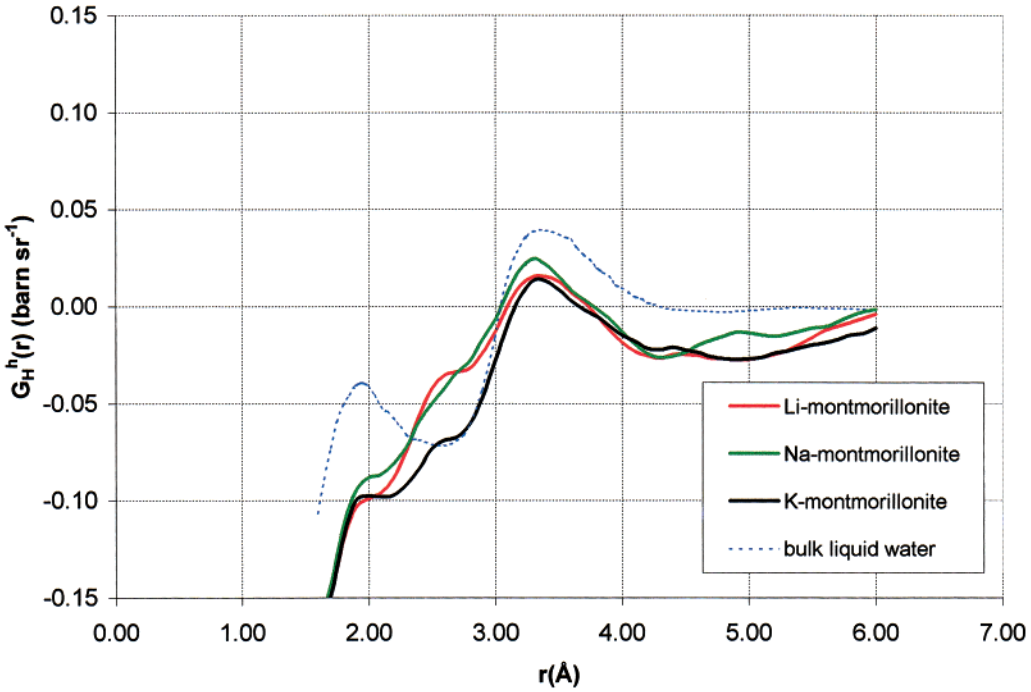

Figure 6. Comparison of $G_H^h(r)$ for Li-, Na-, and K-montmorillonite (solid lines) with a scaled $G_H^w(r)$ for bulk liquid water obtained with eq 5 using neutron diffraction data[16] (dashed lines).

$G_H^w(r) \approx 0$). The 2-Å peak difference likely reflects more extensive hydrogen bonding in the bulk liquid (cf. the N_{HO} values in Table 4), which is not disrupted by cation solvation shells or by the influence of clay mineral surface oxygens. Figure 6 also shows that the simulated $G_H^h(r)$ of interlayer water in the two-layer hydrate of Li-montmorillonite is virtually identical with that of Na-montmorillonite. Minimal differences between the two $G_H^h(r)$ are observed even at $r \approx 3.3$ Å, where second-shell H−O correlations are observed. However, for 2 Å $< r <$ 3.8 Å, the K-montmorillonite hydrate shows dramatic differences in $G_H^h(r)$ from the other two, indicating that the local ordering of water molecules contributing to first-shell (1.9 Å) and second-shell H−O (3.3 Å) spatial correlations is also significantly different. Evidently, the disrupted water structure is different because the counterions within the interlayer are solvated differently. The sharp deviation of $G_H^h(r)$ for interlayer water in K-montmorillonite from the other two interlayer water $G_H^h(r)$ values is indeed striking and worthy of experimental confirmation.

4. Conclusions

We have investigated the interlayer molecular structure in Li-, Na-, and K-montmorillonite hydrates through Monte Carlo simulations of the total radial distribution function. Our simula-

tion results for the two-layer hydrates of Na- and Li-montmorillonite were in good agreement with available experimental data based on isotopic-difference neutron diffraction experiments[8−10] but were not similar to a first-order difference total radial distribution function based on experimental partial radial distribution functions for bulk liquid water.[16] The principal cause of this discrepancy lies with hydrogen−oxygen and hydrogen−hydrogen spatial correlations, which differ significantly among the interlayer water molecules from what occurs in the bulk liquid. Moreover, as indicated in Figures 1−3, oxygen−oxygen spatial correlations are longer-ranged in interlayer water, evidently because of Na^+ and Li^+ solvation effects. By contrast, strong H−O and H−H spatial correlations were absent in the two-layer hydrate of K-montmorillonite, and its simulated first-order difference total radial distribution function differed considerably from those for the Na- and Li-montmorillonite hydrates. This prediction could be checked by performing isotopic-difference neutron diffraction experiments for the K-montmorillonite hydrate like those reported by Powell et al.[8−10]

Acknowledgment. The research reported in this paper was supported in part by the Director, Office of Energy Research, Office of Basic Energy Sciences, of the U.S. Department of Energy under Contract No. DE-AC03-76SF00098. The authors express gratitude to the National Energy Research Scientific Computing Center for allocations of time on its Cray J90 supercomputers. The authors also thank Rebecca Sutton for providing primordial MC results on the K-montmorillonite hydrate, Hugh Powell and Cédric Pitteloud for providing their experimental total RDFs for Li- and Na-montmorillonite, Alan Soper for providing his experimental results on the partial RDFs for bulk liquid water, and Angela Zabel for excellent preparation of the typescript.

References and Notes

(1) Güven, N. *Rev. Mineral.* **1989**, *19*, 497−559.

(2) Sposito, G. *The Surface Chemistry of Soils*; Oxford University Press: New York, 1984; Chapters 2 and 3.

(3) (a) Boek, E. S.; Coveney, P. V.; Skipper, N. T. *J. Am. Chem. Soc.* **1995**, *117*, 12608−12617. (b) Boek, E. S.; Coveney, P. V.; Skipper, N. T. *Langmuir* **1995**, *11*, 4629−4631.

(4) Parker, A. *Clays and the Environment*; Springer: New York, 1998.

(5) Sposito, G.; Prost, R. *Chem. Rev.* **1982**, *82*, 553−573.

(6) (a) Enderby, J. E.; Neilson, G. W. *Rep. Prog. Phys.* **1981**, *44*, 620. (b) Neilson, G. W.; Enderby, J. E. *Adv. Inorg. Chem.* **1989**, *34*, 195−218.

(7) Ohtaki, H.; Radnai, T. *Chem. Rev.* **1992**, *92*, 1157−1204.

(8) Powell, D. H.; Tongkhao, K.; Kennedy, S. J.; Slade, P. G. *Clays Clay Miner.* **1997**, *45*, 290−294.

(9) Powell, D. H.; Tongkhao, K.; Kennedy, S. J.; Slade, P. G. *Physica B* **1998**, *241*−*243*, 387−389.

(10) Powell, D. H.; Fischer, H. E.; Skipper, N. T. *J. Phys. Chem. B* **1998**, *102*, 10899−10905.

(11) Nomenclature suggested by Dr. A. K. Soper, ISIS Neutron Division, Rutherford Appleton Laboratory, Chilton, Didcot, England. Personal communication, 1998.

(12) Beveridge, D. L.; Mezei, M.; Mehrootra, P. K.; Marchese, F. T.; Ravi-Shanker, G.; Vasu, T.; Swaminathan, S. In *Molecular-Based Study of Fluids*; Haile, J. M., Mansoori, G. A., Eds.; American Chemical Society: Washington, DC, 1983; pp 297−351.

(13) Sposito, G.; Park, S.-H.; Sutton, R. *Clays Clay Miner.* **1999**, *47*, 192−200.

(14) Chang, F.-R. C.; Skipper, N. T.; Refson, K.; Greathouse, J. A.; Sposito, G. In *Mineral-Water Interface Reactions*; Sparks, D. L., Grundl, T., Eds.; American Chemical Society: Washington, DC, 1998; Chapter 6.

(15) Sears, V. F. *Neutron News* **1992**, *3*, 29−37.

(16) Soper, A. K.; Bruni, F.; Ricci, M. A. *J. Chem. Phys.* **1997**, *106*, 247−254.

(17) Skipper, N. T.; Chang, F.-R. C.; Sposito, G. *Clays Clay Miner.* **1995**, *43*, 285−293.

(18) Chang, F.-R. C.; Skipper, N. T.; Sposito, G. *Langmuir* **1998**, *14*, 1201−1207.

(19) Chang, F.-R. C.; Skipper, N. T.; Sposito, G. *Langmuir* **1997**, *13*, 2074−2082.

(20) Matsuoka, O.; Clementi, E.; Yoshimine, M. *J. Chem. Phys.* **1976**, *64*, 1351−1361.

(21) Bounds, D. G. *Mol. Phys.* **1985**, *54*, 1335−1355.

(22) Kusalik, P. G.; Svishchev, I. M. *Science* **1994**, *265*, 1219−1221.

(23) The values of N_{OO} and r_{min} for MCY bulk liquid water are not significantly different from the experimental values.[13]

(24) Sposito, G.; Skipper, N. T.; Sutton, R.; Park, S.-H.; Soper, A. K.; Greathouse, J. A. *Proc. Natl. Acad. Sci. U.S.A.* **1999**, *96*, 3358−3364.

(25) The experimental data in Figure 5 are based on very recent neutron diffraction data for the two-layer hydrate of Na-montmorillonite (Powell, H. and Pitteloud, C. Institut de Chimie Minérale et Analytique, Université de Lausanne-BCH. Personal communication, 1999). They are comparable to the data of Powell et al.[8]